

# PHOTON RECYCLING IN THIN-FILM GaAs SOLAR CELLS

**Natasha Gruginskie** – n.gruginskie@science.ru.nl

**Gerard J. Bauhuis** – g.bauhuis@science.ru.nl

**Peter Mulder** – p.mulder@science.ru.nl

**Elias Vlieg** – e.vlieg@science.ru.nl

**John J. Schermer** – j.schermer@science.ru.nl

Radboud University, Institute for Molecules and Materials, Applied Materials Science.

Heyendaalseweg 135, 6525 AJ Nijmegen, The Netherlands

**Abstract.** *The highest efficiencies in single-junction solar cells are obtained with devices based on GaAs. As this material is reaching the limit in material quality, the optimization of the design of the cell becomes more important. In this study we implement a patterning technique to the bottom contact layer of thin-film GaAs solar cells that increases the reflectance of photons to the active layers. Both shallow junction and deep junction devices were evaluated, and the area of the rear side of the cells covered by the contact layer was varied from 100% to 10%. With the patterning, a clear increase in reflectance can be observed for both geometries, but an improved performance was only seen in deep junction devices. For these cells, both the short circuit current and the open circuit voltage increase with the reflectance. Dark curve analysis demonstrated a reduction in the radiative saturation current density, indicating that the observed increase in the open circuit voltage is a result of increased photon recycling.*

**Keywords:** *Gallium arsenide, Thin-film solar cells, Photon recycling.*

## 1. INTRODUCTION

Currently, there are many types of existing solar cells ranging from single layer organic solar cells, to monocrystalline multi-junction solar cells based on III-V materials (Green *et al.*, 2017; NREL, 2017). The different cell types differ enormously in cost and efficiency. Generally, the higher the efficiency of a solar cell, the more expensive it is. At present, virtually all the commercially available solar panels contain single-junction solar cells composed of either Silicon (Si), Copper-Indium-Gallium-Selenide/Sulfide (CIGS) or Cadmium-Telluride (CdTe), with efficiencies ranging between about 8 and 20%. Significantly higher efficiencies of over 40% have been demonstrated with solar cells based on III-V materials. The group of III-V materials are formed by a one-to-one combination of elements from the third (mostly aluminum, gallium and indium) and the fifth (mostly phosphorous, arsenic and nitrogen) column of the periodic table. These cells are not yet applied in consumer modules because of their high cost. For this reason, they are at present mainly utilized in satellites and space exploration purposes, where the high launch costs cause the high efficiency of the III-V solar cells to outweigh their high price.

Another application where the high efficiency of the III-V solar cells can outweigh their high price is a so-called concentrator system. A concentrator system basically collects sunlight over a large area and focuses it on a solar cell with a much smaller surface area. This way, the size of the solar cell that is required to produce a certain power output can be reduced by several orders of magnitude. The fact that the required optics are substantially cheaper per unit area than the solar cells allows for a reduction in the cost per watt output power for photovoltaic energy. Since the solar cell in such applications only amounts to a small part of the total system costs, III-V solar cells are the most economical choice at sufficiently high concentration ratios. In this scenario, multi-junction solar cells composed mainly by Indium Gallium Phosphide (InGaP), Gallium Arsenide (GaAs) and Germanium (Ge) sub-cells are widely used, as they can be tuned to absorb a wider wavelength range from the incident light. Contemporary research in general aims to increase the efficiency in these systems by i) optimizing the amount and position of sub-cells in multi-junction devices and ii) increasing the efficiency of each sub-cell towards its theoretical maximum. In this respect this study will focus on mechanisms that allow the production of single junction GaAs solar cells with efficiencies closer to their theoretical efficiency limit.

## 2. III-V MATERIALS FOR SOLAR CELLS

The semiconductor industry heavily relies on silicon, mostly because it is able to form a very controllable electrically insulating oxide layer and because the material is abundantly available in nature, and therefore inexpensive. For many applications, like micro-electronic circuitry, these qualities are favorable. However, silicon is an indirect band-gap material and for opto-electronic circuits, semiconductors with direct bandgaps, such as III-V materials, are required in order to obtain good and efficient working devices. In addition, III-V materials have the advantage that by changing the fractions of each element, while keeping the one-to-one ratio between third and fifth column elements constant, many

semiconductors properties, like bandgap, lattice constant, chemical stability, etc. can be tuned. Furthermore, certain elements like zinc, carbon or silicon, can be easily added during formation of the III-V material resulting in highly controllable  $p$ - an  $n$ - type doping levels. However, III-V materials have the disadvantage that they are not able to form a stable and controllable oxide layer and most of the materials are relatively expensive because they are not explored at large scale. Crystal growth techniques like liquid encapsulated Czochralski (LEC) growth, horizontal Bridgeman (HB) method or the vertical gradient freeze (VGF) method are often employed for fabricating high quality III-V materials crystals. These methods are usually only used for binary III-V compounds like GaAs and InP, because with these techniques the control of the composition for ternary or more complicated compounds is very difficult. The large crystal ingots or boules obtained in this way are usually cut into wafers. Subsequently these wafers are used as substrates or templates to produce epitaxial solar cell structures utilizing crystal growth methods that allow for close control of the material composition. Common epitaxy techniques are liquid phase epitaxy (LPE), molecular beam epitaxy (MBE), metal organic chemical vapor-phase deposition (MOCVD) or combinations of these techniques. In general, a thin layer or stack of layers in the order of a few micrometers is deposited on a substrate that should approximately have the same lattice constant, in order to obtain a virtually perfect single-crystalline structure. The MOCVD growth technique also allows the growth of lattice-matched passivating layers on top and bottom of the solar cell structure, with a slightly larger band gap than the solar cell material. Due to this difference in band gaps, electric fields are induced at the surfaces, these fields repel the minority carriers and thereby reduce the recombination rate at the surfaces.

The high production costs of III-V devices is mainly caused by the price of the substrates that are necessary to obtain the generally desired single crystal layer structures or devices. Once a device is grown, the substrate usually does not have a function other than being an expensive carrier of the device structure. On the other hand, the most frequently used materials for these cells such as GaAs and InGaP are direct band gap semiconductors with high absorption coefficients. Therefore, a stack with a thickness of only a few micrometers of these materials is required to absorb all light that the solar cell can convert into electricity. There are several methods for removal of the growth substrate, resulting in thin-film solar cells. By a selective etching process, the complete substrate can be removed using an etch stop layer that protect the solar cell layers. Another method is the Epitaxial Lift-Off (ELO) technique in which the thin-film III-V structures are separated from their wafer template so that the latter can be reused for growth of the next thin-film cell structure. In both cases, the actual thin-film structures are transferred to a low cost foreign carrier like a metal or plastic foil for stability and further processed into a genuine thin-film cell.

Thin-film cells have several application advantages over cells on a substrate. First, the final devices are thinner and thus lighter, which results in severe launch costs reduction for space applications. Second, the thin cells are better resistant against cosmic radiation. The cosmic particles often do not damage the solar cell itself, but penetrate it to form defects in the substrate on which the solar cell is grown. These defects propagate upwards and deteriorate the cell performance. In a thin-film cell, most cosmic particles might simply pass through the cell without damaging it. Third, the cells can be mounted on an arbitrary carrier, like a low weight material for space applications, another low-bandgap solar cell to form a mechanically stacked tandem solar cell (Schermer *et al.*, 2006), or a good heat conductor in concentrator applications.

### 3. THIN-FILM GaAs SOLAR CELLS

The most suitable III-V material for a single junction solar cell is GaAs, since it has the optimal bandgap to achieve high energy conversion rates and it has shown the highest conversion rate among all types of single junction solar cells (Yang *et al.*, 2014). As shown in Fig.1, the world record for single-junction thin-film GaAs solar cells was first achieved by Radboud University in 2005, with an efficiency of 24.5% (Green *et al.*, 2005), and a few years later this geometry reached the efficiency from the substrate based cell of 26.1% (Bauhuis *et al.*, 2009). The current world record of 28.8% was achieved by Alta Devices in 2012, and it is 2.3% higher than the current record for substrate based (Green *et al.*, 2017). Because this efficiency has not been surpassed to date, it is safe to assume that this material is very close to the limit in material quality and the design of the cells becomes a determinant parameter in order to further increase the performance of these cells.

The typical structure for a single junction solar cell has a shallow junction (SJ) design, with a thin highly doped  $n$ -type emitter and a thick lightly doped  $p$ -type base. However, Steiner *et al.* (2013) have demonstrated an increase in thin-film cell efficiency, mainly as a result of a higher open-circuit voltage ( $V_{oc}$ ), using a deep junction (DJ) design with a thick, lightly doped emitter and a thin highly doped base layer. The high  $V_{oc}$  values that were obtained in the latest thin-film GaAs solar cells indicate an increase in the external radiative efficiency of the cell (Kosten *et al.*, 2011). In the thin-film structure, radiatively emitted photons are reflected from a metallized back surface instead of being absorbed in the substrate, resulting in the large increase in  $V_{oc}$ . Because GaAs is a good absorber but also a very good emitter, the high internal emission in DJ devices makes the optical design of the final devices to be extremely important, and theoretical studies indicate that improvements in the back-side mirror reflectivity to a level beyond 95% will further increase the cell efficiency super-linearly (Miller *et al.*, 2012). Because the light absorption rate and related carrier generation decrease exponentially with the distance from the surface, the collection efficiency in the upper part of the solar cell has a strong impact on the generated short-circuit current density ( $J_{sc}$ ). Therefore, for the production of good quality DJ devices, besides a high back side reflectivity, also the diffusion length of the minority carriers in the thick emitter is a critical parameter (Bauhuis *et al.*, 2016).

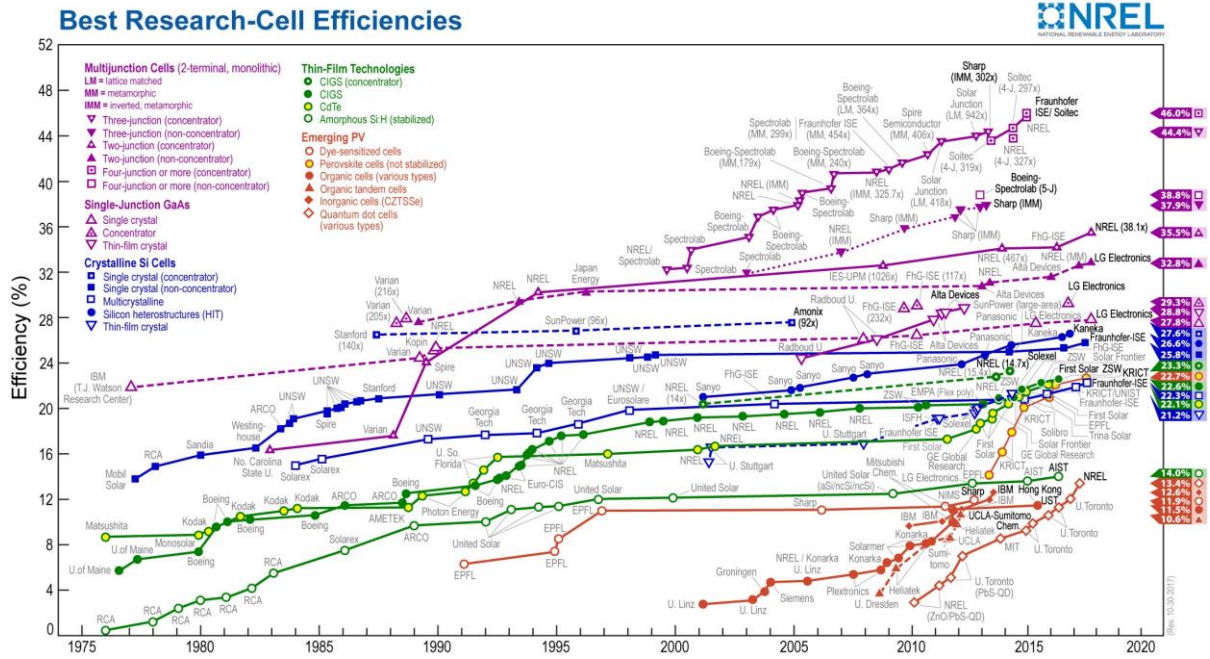


Figure 1 - Best research-cell efficiency chart, displaying the highest solar cells efficiencies measured for different solar cell technologies (NREL, 2017).

A schematic depiction of the most commonly used growth structure and of the completely processed design are shown in Fig. 2. In the current state of developing thin-film GaAs solar cells, both by ELO or by chemically removing the substrate, the result is a structure with passivating phosphide layers on top and bottom of the *pn*-junction, and the first and last layers are highly doped GaAs contact layers, responsible for a good ohmic contact. The front and rear metal contacts are gold and the structure is mounted on a Cu metal carrier. In between the grid fingers in the front contact, the contact layer is etched away to avoid parasitic absorption of light, but in the rear side it remains whole.

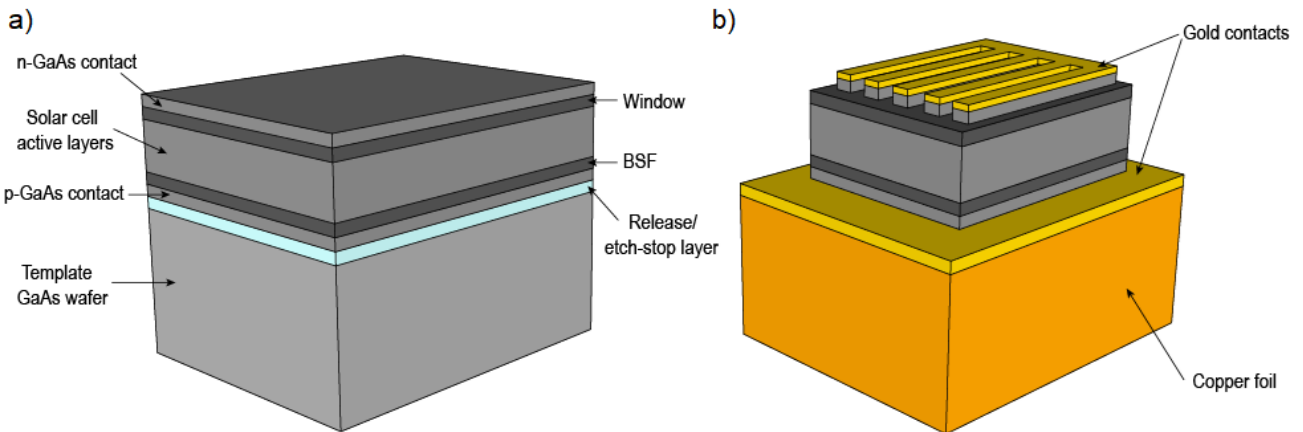


Figure 2 - Schematic depiction of a) the structure of a solar cell after deposition of the epitaxial layers and b) of the final device after processing into an actual thin-film device. Images not to scale.

The bottom contact layer in the thin-film configuration, however, is highly doped GaAs, which absorbs a large portion of the photons below the bandgap energy. This can prevent a significant fraction of the radiatively emitted photons to be recycled by absorption in the active layers of the cell (Gruginskie *et al.*, 2017), because photons absorbed in the passivating and contact layers do not contribute to the solar cell performance. To circumvent this loss mechanism we will with this study implement a patterning process to the p-GaAs contact layer that increases the reflectance in the radiative emission wavelength region in both SJ and DJ solar cells and compare the differences in performance of both structures.

#### 4. EXPERIMENTAL TECHNIQUES

The cells were grown using low-pressure MOCVD on 2 inch GaAs wafers with (1 0 0)  $2^\circ$  off to [1 1 0] orientation. In this work, two junction depths were tested: a SJ design with a 75 nm thick emitter and a 2000 nm base, and a DJ design with a 2000 nm emitter and a 75 nm base. Before growth of the actual solar cell structure, a 150nm thick AlInGaP etch-stop layer was grown in order to limit the etching of the wafer. The wafer was etched in a citric acid/hydrogen peroxide solution for approximately 2 hours and subsequently the etch-stop layer was removed with HCl 37%. The now exposed p-contact layer was patterned by photolithography, as illustrated in Fig. 3, and etched in an ammonia/hydrogen peroxide solution. Each 2 inch wafer was patterned into cells with 3 different rear surface area coverages ( $C_r$ ) of 100%, 30% and 10%. On the etched areas, 60 nm of ZnS was applied by thermal evaporation and the rear metal contact was e-beam evaporated continuously, so at the etched areas it will function as a mirror. The final structure was mounted on a copper foil that serves as a conducting, flexible and stable carrier.

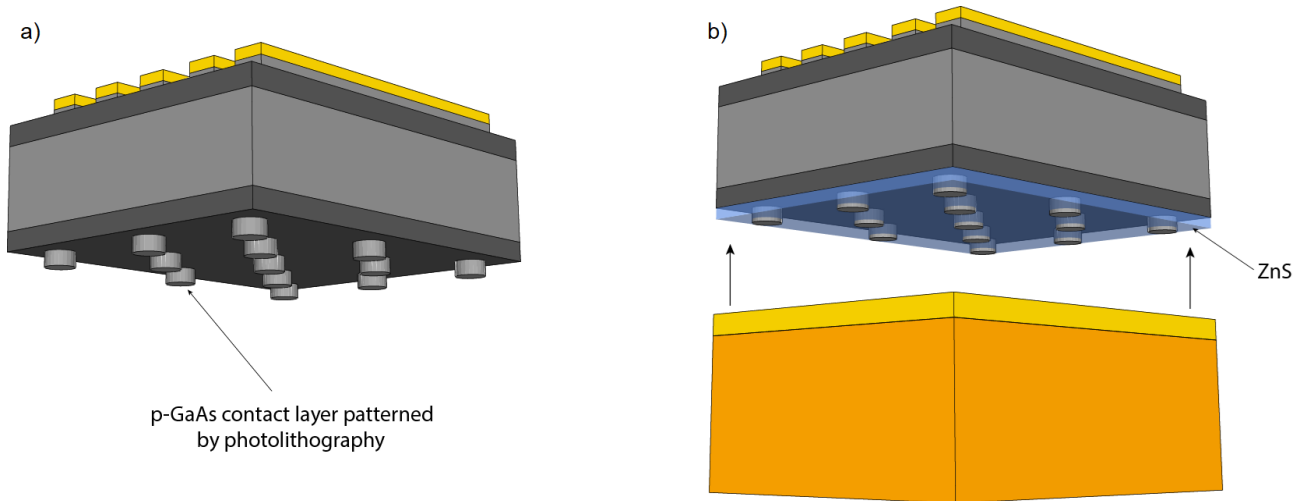


Figure 3 - Schematic depiction of the rear contact pattern process applied to the p-GaAs contact layer in a 2 inch wafer. a) Structure after patterning the back contact layer, b) after filling the removed contact area with ZnS just before application of the metal foil reflector/carrier.

For probing convenience, a relatively large frontal grid coverage of 16.6% was applied, also by e-beam evaporation.  $5 \times 5 \text{ mm}^2$  solar cells were defined by a MESA etch, using an ammonia/hydrogen peroxide solution for the GaAs layer and a bromide solution for the phosphide layers. The *n*-GaAs contact layer was removed in between the grid fingers also with an ammonia/hydrogen peroxide solution, and an anti-reflection coating consisting of 94 nm of ZnS and 44 nm of  $\text{MgF}_2$  was deposited by thermal evaporation.

After processing, I-V curves of the cells were measured under AM1.5G conditions ( $1000 \text{ w/cm}^2$  at  $25^\circ\text{C}$ ) using a Keithley 2600 multimeter with an Abet Xe light source. The data acquisition software ReRa Tracer 3 was used and a calibrated reference cell was used to correct for the deviation in irradiation. Dark I-V curve characteristics were composed from  $J_{sc}$ - $V_{oc}$  values measured under different light intensities to avoid series resistance effects at higher current levels (Bauhuis *et al.*, 2016). The reflectance measurements were performed using a FilMetrics spectrophotometer perpendicular to the analyzed surfaces.

#### 5. RESULTS AND DISCUSSIONS

The effect that the partial removal of the contact layer has in the total reflectance of the produced solar cells was measured with a spectrophotometer. With this technique the reflectance is measured at the front surfaces of the cell. Because below the bandgap wavelength basically all the light is absorbed in the material, only the behavior of the longer wavelength range of the incident light can be analyzed. The reflectance in this region is, however, a good indication of the reflectance just below the bandgap wavelength. Fig. 4 shows the obtained reflectance curves, and it shows that for both SJ and DJ devices there is a large increase in the total reflectance with decreasing rear contact coverage.

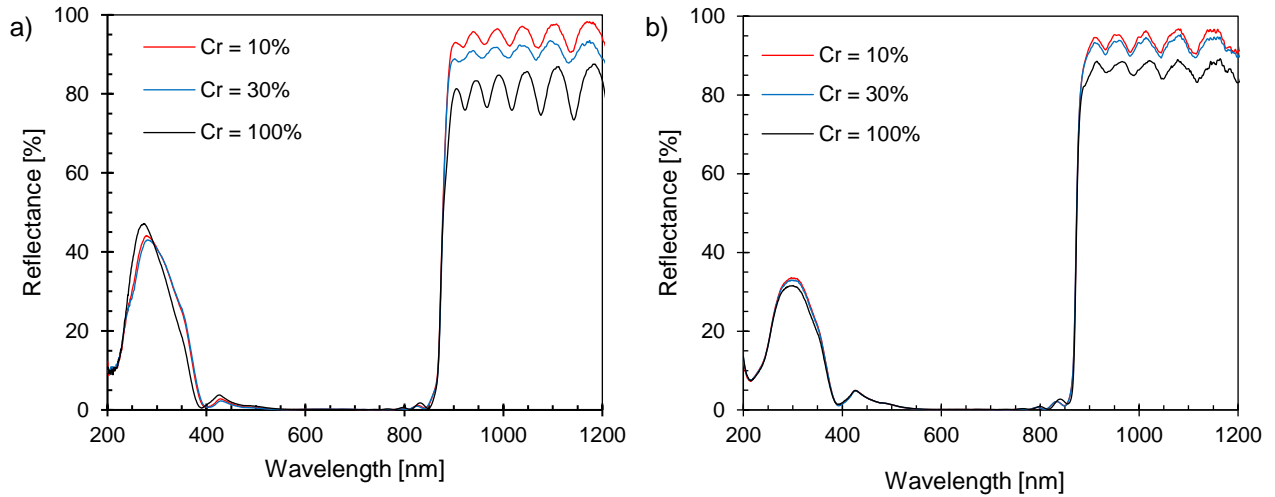


Figure 4 - Measured wavelength dependent reflectance of a) SJ and b) DJ solar cells with different  $C_r$  values.

The illuminated J-V curves of the produced solar cells are presented in Fig. 5, and the parameters values corrected for shading losses from the front grid are stated in Tab.1. The shape of the J-V curves indicates that the patterning of the rear side has an overall detrimental effect to the shallow junction configuration for both  $C_r = 30\%$  and  $C_r = 10\%$ . For the DJ cells, however, only for  $C_r = 10\%$  the fill factor (FF) decreases due to series resistance effects.

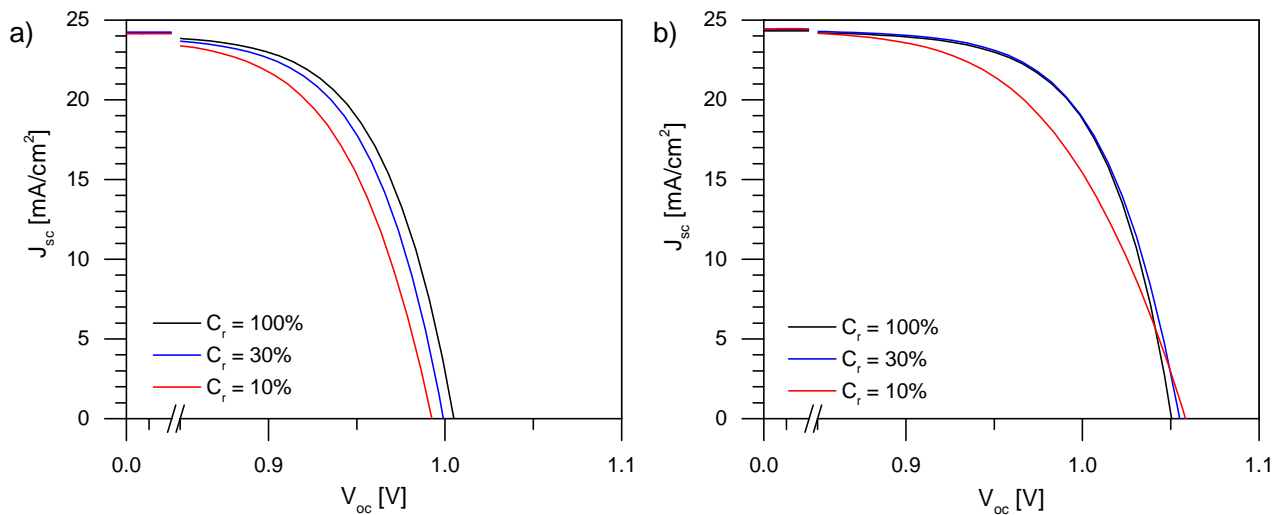


Figure 5 - Illuminated J-V curves of a) SJ and b) DJ solar cells with different  $C_r$  values.

In the SJ devices, the  $J_{sc}$  values remain almost constant, but both the  $V_{oc}$  and the FF decrease as  $C_r$  decreases. The back-side pattern offers no advantage to this geometry. For the DJ solar cells, however, there is a mild increase in  $J_{sc}$  of  $0.15 \text{ mA/cm}^2$  and a more than linear increase in  $V_{oc}$  up to 8 mV. The fill factor, however, has a reduction of 3.4% from  $C_r = 30\%$  to  $C_r = 10\%$ . Because the rear contact consist of a thin Au layer and a thick Cu foil, contact resistances effects can be disregarded, and the fill factor drop is associated to a large lateral resistance that carriers face from the point they are generated to the contact points. In follow up research this effect can be easily circumvented with a more evenly distributed contact pattern, consisting in smaller contact areas placed closer to each other.

Table 1 - Illuminated J-V parameters with  $J_{sc}$  corrected for shading losses from the front metal contacts of both SJ and DJ solar cells with different rear surface contact fractions.

$C_r$ [%]	SJ devices				DJ devices			
	$J_{sc}$ [mA/cm <sup>2</sup> ]	$V_{oc}$ [mV]	FF [%]	$\eta$ [%]	$J_{sc}$ [mA/cm <sup>2</sup> ]	$V_{oc}$ [mV]	FF [%]	$\eta$ [%]
100	28.99	1006	85.0	24.84	29.18	1050	85.8	26.29
30	29.06	999	84.4	24.53	29.29	1055	85.5	26.42
10	28.96	992	83.6	24.01	29.33	1058	82.1	25.46

Applying forward bias to a solar cell in the dark will generate a recombination current density  $J_{rec}$  that can be approximated by two diodes in parallel, and is described by:

$$J_{rec} = J_{01} \left( e^{\frac{qV}{kT}} - 1 \right) + J_{02} \left( e^{\frac{qV}{2kT}} - 1 \right), \quad (1)$$

where  $J_{01}$  is the saturation current density of the  $n=1$  component and  $J_{02}$  is the saturation current density of the  $n=2$  component. The ratio between the two components of the recombination current is voltage dependent, with non-radiative recombination dominating  $J_{rec}$  at low voltages (the  $n=2$  region) and radiative recombination dominating at higher voltages (the  $n=1$  region).

The generated dark current of both SJ and DJ solar cells with  $C_r = 100\%$  are shown in Fig. 6a, with the  $n=1$  and  $n=2$  slope highlighted. The fitted values for  $J_{02}$  are  $1.5 \times 10^{-11}$  A/cm<sup>2</sup> for the SJ cell and  $4.7 \times 10^{-12}$  A/cm<sup>2</sup> for the DJ cell. For the increase in reflectance to have sufficient impact on the performance of the cells by an increase in the  $V_{oc}$ ,  $J_{02}$  has to be sufficiently low so that  $J_{01}$  configures a larger fraction of  $J_{rec}$ . The fact that the SJ device exhibits a  $J_{02}$  value that is one order of magnitude higher than that of the DJ cells shows that at operating voltage  $J_{rec}$  of the SJ cell is mostly non-radiative.

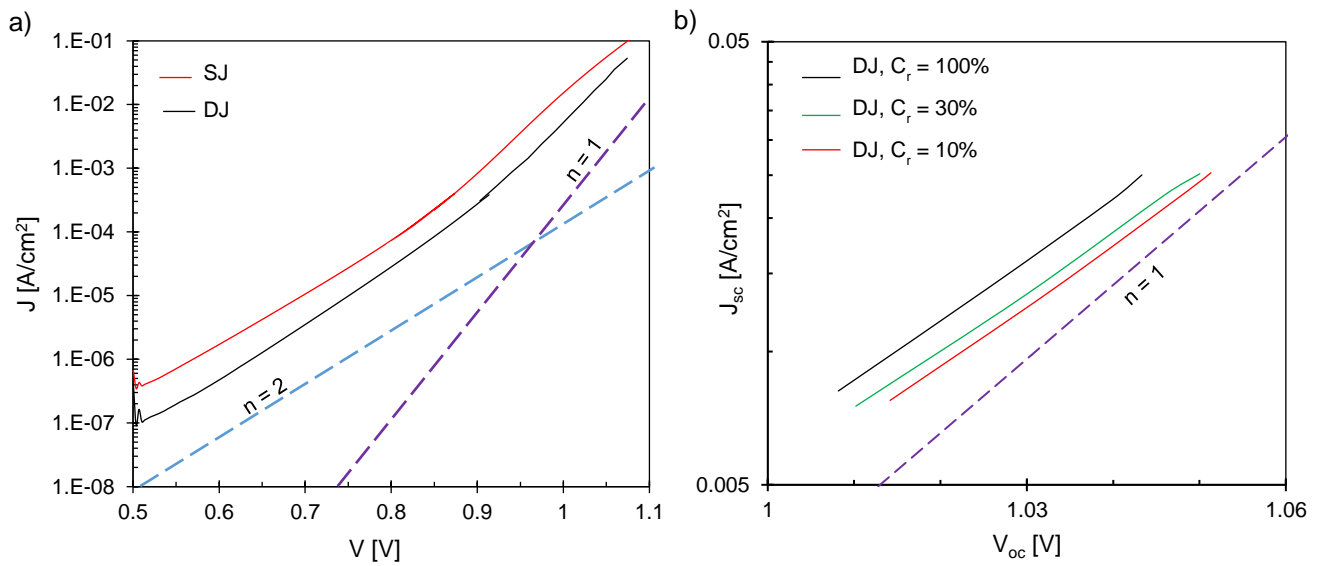


Figure 6 - a) Dark I-V curves of the SJ and DJ solar cells with  $C_r = 100\%$  and b)  $J_{sc} - V_{oc}$  curves of the DJ cells with different  $C_r$  values.

Because at higher voltages the series resistances of the cells influences  $J_{rec}$ , leading to a curve bent downwards, the  $J_{sc} - V_{oc}$  curves are used to determine  $J_{01}$  of the DJ solar cells with different  $C_r$ , shown in Fig. 6b. The decrease in the  $J_{01}$  value from  $8.8 \times 10^{-20}$  A/cm<sup>2</sup> for  $C_r = 100\%$  to  $6.0 \times 10^{-20}$  A/cm<sup>2</sup> for  $C_r = 10\%$  confirms that the increase in voltage is indeed a result of a more efficient reabsorption of emitted photons.

It has been previously stated that thin-film solar cells can only achieve efficiencies closer to 30% in a deep junction geometry (Bauhuis *et al.*, 2016), and the results showed in this work corroborate to this suggestion. The production of good quality single crystalline epitaxial cells with a deep junction and high internal emission combined with a well-designed rear mirror have the potential to achieve efficiencies close to the theoretical limit of 33.5% (Miller *et al.*, 2012).

## 6. CONCLUSION

In this study, the effect of the junction depth and the reflectance of the bottom layers in thin-film GaAs solar cells was evaluated. A patterning approach that partially removes the absorbing contact layer and increases the rear side reflectance was applied to both shallow junction and deep junction solar cells. The processing of solar cells with different  $C_r$  on the same growth wafer allowed for direct comparison between the applied geometries. The resulting solar cells exhibited an increase of more than 20% in reflectance of the incident light for wavelengths just above the band-gap at the lowest  $C_r$  value.

The effect of the patterning was found to be detrimental for the performance of the SJ devices, presenting a decrease in the  $V_{oc}$  and FF, even though the reflectance was increased. For the DJ devices, however, both  $J_{sc}$  and  $V_{oc}$  increased with decreasing  $C_r$  values. The dark current analysis suggests that the differences in performance is due to a much larger non-

radiative saturation current density in the SJ devices. The consistent reduction in  $J_{01}$  of the DJ cells demonstrate that the increased  $V_{oc}$  is a result of improved photon recycling inside the cell. For the  $C_r = 10\%$  cell, however, the high lateral resistance resultant from the long distance between contact points causes the FF values to drop in 3%, reducing the efficiency.

The results in this study experimentally confirm the previously reported relationship between the reflectance of the rear contact and the parameters of thin-film GaAs solar cells. Furthermore, it was shown that the deep junction geometry is required in order to produce devices with high internal emission, which allows the dark current to be further reduced without changes to the active cell structures. The presented concept of a discontinuous rear contact together with further reduction of the non-radiative losses at the perimeter of the cells represent a viable approach to produce single junction GaAs solar cells with efficiencies closer to 30%.

### **Acknowledgements**

The authors acknowledge financial support from the Brazilian National Council for Scientific and Technological Development (CNPq), under the program Science without Borders, project 233259/2014-7.

### **REFERENCES**

- Green, M.A., Hishikawa, Y., Warta, W., Dunlop, E.D., Levi, D.H., Hohl-Ebinger, J., Ho-Baillie, A.W.H., 2017. Solar cell efficiency tables (version 50), *Prog Photovolt Res Appl.* 2017; 25:668–676.
- National Renewable Energy Laboratory (NREL), “Best Research-Cell Efficiencies”. <https://www.nrel.gov/pv/assets/images/efficiency-chart.png>, 2017 [Online; accessed in 16.11.2017].
- Schermer, J.J., Bauhuis, G.J., Mulder, P., Haverkamp, E.J., van Deelen, J., van Niftrik, A.T.J., Larsen, P.K., 2006. Photon confinement in high efficiency, thin-film III-V solar cells obtained by epitaxial lift-off, *Thin Solid Films* 511-512 (2006) 645-653.
- Yang, W., Becker, J., Liu, S., Kuo, Y., Li, J., Landini, B., Campman, K., Zhang, Y., 2014. Ultra-thin GaAs single-junction solar cells integrated with a reflective back scattering layer, *J. Appl. Phys.* 115, 203105 (2014).
- Green, M. A., Emery, K., King, D.L., Igari, S., Warta, W., 2005. Solar Cell Efficiency Tables (Version 26), *Prog. Photovolt: Res. Appl.* 2005; 13:387–392.
- Bauhuis, G.J., Mulder, P., Haverkamp, E.J., Huijben, J.C.C.M., Schermer, J.J., 2009. 26.1% thin-film GaAs solar cell using epitaxial lift-off, *Solar Energy Materials & Solar Cells* 93 (2009) 1488-1491.
- Steiner, M. A., Geisz, J. F., Garcia, I., Friedman, D. J., Duda, A., Kurtz, S. R., 2013. Optical enhancement of the open-circuit voltage in high quality GaAs solar cells, *J. Appl. Phys.* 113, 123109 (2013).
- Kosten, E.D., Kayes, B.M., Atwater, H.A., 2011. Experimental demonstration of enhanced photon recycling in angle-restricted GaAs solar cells, *Energy Environ. Sci.* 2011, 1907-1912.
- Miller, O.D., Yablonovitch, E., Kurtz, S.R., 2012. Strong internal luminescence as solar cells approach the Schokley-Queisser limit, *IEEE Journal of Photovoltaics*. Vol 2. No 3, July 2012.
- Bauhuis, G., Mulder, P., Hu, Y., Schermer, J., 2016. Deep Junction III-V solar cells with enhanced performance, *Phys. Status Solidi A* 2016, No. 8, 2216—2222 (2016).
- Gruginskie, N., van Laar, S.C.W., Bauhuis, G., Mulder, P., van Eerden, M., Vlieg, E., Schermer, J.J., 2017. Increased performance of thin-film GaAs solar cells by rear contact/mirror patterning. Submitted to *Thin Solid films* in 2017.